Effect of gelatin additive on microstructure and composition of electrodeposited rhenium–nickel alloys in aqueous solutions

Wangping Wu[1]

Abstract Re–Ni alloys with high Re content were electrodeposited galvanostatically from aqueous solutions with addition of gelatin. The influence of gelatin on the Faradaic efficiency (FE), chemical composition, morphology and crystallographic structure of the alloys was investigated. Morphology, surface roughness, chemical composition and phase identification of the alloys were characterized by an environmental scanning electron microscopy, atomic force microscopy, energy-dispersive spectroscopy and X-ray diffraction, respectively. The addition of gelatin in the plating led to the increase in Re content, and the decrease in the FE and deposition rate. In the absence and presence of gelatin, the alloys with high Re content consisted of an amorphous phase. The addition of gelatin resulted in small amount of carbon in the alloys due to the adsorption of gelatin in the alloy. The gelatin had a great influence on the morphology of the alloys, resulting in significant grain coarsening, the increase in surface roughness and the decrease in crack size. The optimum concentration of gelatin was found to be about 0.9–2.7 g L^{-1}.

1 Introduction

The use of organic additives in aqueous electroplating solutions can affect the growth and microstructure of the metal and alloy deposits. Small quantity of organic additives can promote the formation of smooth and shiny deposits. Additive molecules adsorbed on the surface of the cathode can affect the activation energy and the charge transfer rate in the electrochemical reaction, and may also influence the mechanism of electrocrystallization [1–3]. The additives are added to metal plating baths to control hydrogen evolution, crystallization texture, grain size, roughness and growth rate of the deposit, and to reduce residual stress and pitting, and so on [4].

Electrodeposition of rhenium (Re) and its alloys has been reviewed by Eliaz and Gileadi [5]. Electrodeposited Re film has a low Faradaic efficiency (FE) and poor quality. Addition of salts of one of the iron group metals can result in high FE and high Re content, showing a catalytic effect of iron group metals deposition on the electrodeposition of Re [6–9]. Electrodeposition of Re–Ni alloy is of great interest due to the extensive mutual solubility of Re and Ni, the absence of intermetallic compounds in the Re–Ni phase diagram and no phase transformations [7]. The effects of bath composition, pH, temperature, magnetic field and current density on the FE and composition of Re–Ni alloys have been investigated [10–12]. An AFM evaluation of Re–Ni electrodeposition and nucleation on copper (Cu) substrate has been recently presented by Mondal et al. [13]. Further, the unique behavior during the initial stages of Re–Ni alloy was observed [14]. Electrodeposition of Re–Ir–Ni alloys [15] and electroless plating of Re–Ni alloys [16] were studied. However, so far few literatures have been reported on electrodeposited Re–Ni alloy from aqueous solutions with organic additives. Greco [17] reported that fine cracks appeared on the surface of Re–Ni alloy with low Re content (less 16 at.%) electrodeposited with the addition of sodium lauryl sulfate surfactant. Huang et al. [18] studied the Ni–rich Re–Ni alloys electroformed with saccharin additive and found that a crack-free Ni–Re alloy was attained.

✉ Wangping Wu
  wwp3.14@163.com

[1] School of Mechanical Engineering, Changzhou University, Changzhou 213164, People's Republic of China

Electrocrystallization of metals and alloys from aqueous solutions is always accompanied by the generation of stress, which influences the properties of deposits and may cause their cracking and peeling. Gelatin additive, a widely utilized leveling and grain refining agent in electrodeposition of metals and alloys, is known to improve the morphology of deposits, and to control the deposition rate, crystallization, leveling and brightness of the deposit [19]. In this study, the effect of gelatin additive on the FE, the composition, morphology, cracking size and crystallographic structure of Re–Ni alloys with high Re content is to be investigated.

2 Experimental

2.1 Plating bath chemistry

In this experiment, one aqueous solution containing 34 mM NH_4ReO_4, 124 mM $Ni(NH_2SO_3)_2$ and 343 mM $C_6H_8O_7$ was used to produce Re–Ni alloys. Gelatin was used as organic additive. The concentration of gelatin was in range of 0.01–7.0 g L^{-1}. The chemical structure of a short segment of gelatin is shown in Fig. 1. Gelatin contains a high proportion of glycine, almost one in three residues, arranged every third residue, proline and 4-hydroxyproline residues [20].

2.2 Preparation

A three-electrode cell was used. It contained a Cu disk cathode serving as working electrode with an exposed surface area of 1.57 cm^2, two platinum sheets counter-electrode placed at about 0.5 cm away from both sides of the cathode and a Ag/AgCl (saturated KCl) reference electrode. Prior to electroplating, the Cu substrate was cleaned with a detergent in an ultrasonic bath for 5 min in order to remove major contaminants and then immersed in a 1:1 nitric acid at room temperature for about 1 min to remove the native oxide films on the surface of Cu substrate. This was followed by cleaning in the ultrasonic bath for 3–5 min. The deposition conditions of Re–Ni alloy were: pH 5 ± 0.1, bath temperature 70 ± 0.05 °C, current density 50 mA cm^{-2} and deposition time 60 min. The volume of electrolyte in the cell was about 10 mL. A Princeton Applied Research model 263A potentiostat/galvanostat was used to control the applied current density and to perform cyclic voltammetry (CV) conducted at 50 mV s^{-1}. A MRC B300 thermostatic bath was used to control the chosen temperature. All solutions were dissolved in deionized water (Simplicity TM, Millipore). A 5M sodium hydroxide (NaOH) solution was used to adjust to pH values. The bath was purged with pure nitrogen for about 15 min before turning on the current. Nitrogen was passed above the solution during deposition. A magnetic stirrer bar was used to stir the solution in order to maintain homogeneity of the solution and reduce pitting.

The added mass of the specimen was weighed by BA 210 (Sartorius) analytical balance (resolution 0.1 mg) before and after each experiment. The chemical composition of the alloy was measured by energy-dispersive spectroscopy (EDS). The average FE was calculated from the gained mass, the charge passed and the chemical composition of the alloy. The partial current densities were calculated from the gained mass and the chemical composition of the alloy. Further details can be found in Ref. [8].

2.3 Characterization

The microstructure and morphology of surface and cross section of the alloys were observed by an environmental scanning electron microscopy operated in the high-vacuum mode (ESEM, Quanta 200 FEG from FEI). The chemical composition of the deposit was examined by the attached liquid-nitrogen-cooled Oxford Si EDS detector. Each sample was tested at five locations to confirm uniformity. The phase identification of the alloy was determined by an
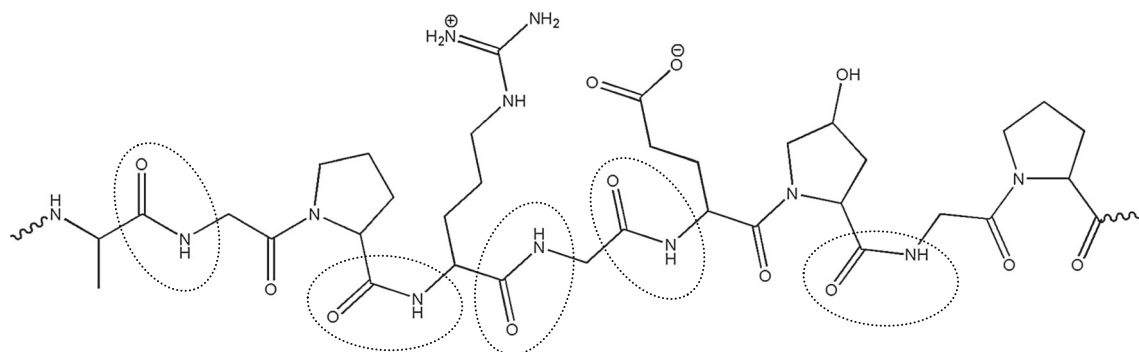

Fig. 1 Chemical structure of a short segment of gelatin (The *dotted lines* is peptide bonds.)

X-ray powder diffractometer (Scintag, USA). The surface roughness of the alloy, including average roughness (R_a) and root mean square roughness (R_q), was characterized by atomic force microcopy (AFM, NT-MDT, Veeco Instruments). The surface roughness of each sample was tested at three locations and averaged.

3 Results

The measured potential of Re–Ni alloys is represented in Fig. 2. The shift of potentials to more negative values was observed with increasing gelatin content in the electrolyte, which was attributed to the adsorption of gelatin onto active growth sites on the surface of cathode, and the increase in solution viscosity with increasing gelatin content. The increase in solution viscosity affected the ability of ion mobility, and finally shifted the potential of electrodeposition toward more negative. In this work, it should be noted that the overpotentials of Re–Ni alloys were kept nearly constant when the gelatin content was above 2.7 g L^{-1}. This indicated that the presence of gelatin affected the deposition process of Re–Ni alloys.

Figure 3 shows the cyclic voltammograms of Cu electrode in aqueous solutions with and without gelatin. The addition of gelatin influenced the overpotential of the deposition, suggesting that the gelatin resulted in the suppression of electrodeposition of Re–Ni alloys. In the presence of gelatin in aqueous solution, the diffusion limiting current density decreased by about 42 mA cm^{-2} compared to no addition of gelatin, due to the preferential adsorption of additive on the cathode surface [21].

The effect of gelatin on behaviors of the alloy is displayed in Fig. 4. The added mass of the samples decreased with increasing gelatin contents, except one maximum value at gelatin content of 0.01 g L^{-1}; further the mass was kept nearly constant when the gelatin content was varied
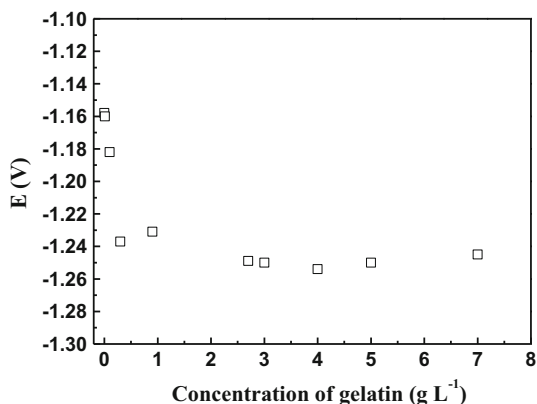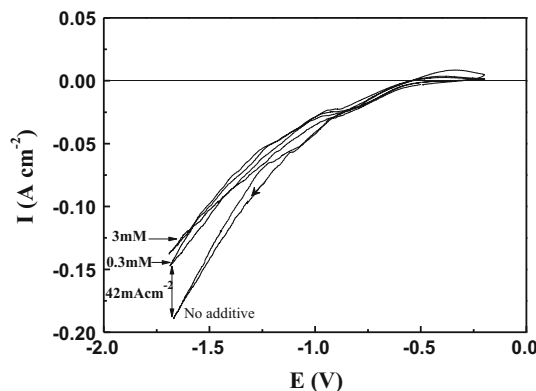

Fig. 3 Cyclic voltammograms of Cu electrode in aqueous solutions with and without gelatin

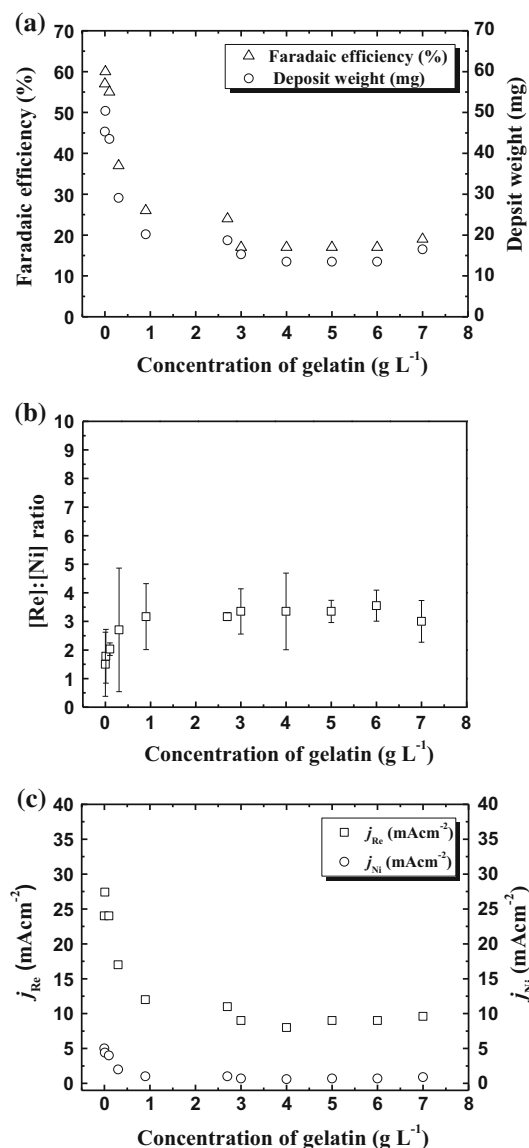**Fig. 4** Effect of gelatin on the FE and the deposit weight (**a**), the [Re]:[Ni] ratio (**b**) and the partial current densities of Re and Ni (**c**)

Fig. 2 Measured potentials of Re–Ni alloys deposited containing different concentrations of gelatin

from 3.0 to 7.0 g L^{-1} (See Fig. 4a). The changed trend of the FE was similar to that of the deposit weight of the samples. The [Re]:[Ni] ratio for Re–Ni alloys is shown in Fig. 4b. The ratio was steadily increased from 1.5 to 3.0 with increasing gelatin contents from 0.0 to 0.9 g L^{-1}, and then increased slightly; further the [Re]:[Ni] ratio was kept almost constant with increasing gelatin contents from 3.0 to 7.0 g L^{-1}. It is evident that the addition of gelatin resulted in an increase in Re content. In Fig. 4c, the partial current densities of Re and Ni markedly decreased with increasing gelatin contents from 0 to 0.9 g L^{-1}, except a maximum value at gelatin content of 0.01 g L^{-1}, and then slightly decreased and further kept nearly constant with increasing gelatin contents.

Figure 5 reveals that the XRD patterns of Re–Ni alloys with and without gelatin. No additive was used; a broad diffraction peak at $\sim 42.6°$ indicated that the alloy was composed of an amorphous phase (Fig. 5a). With increasing gelatin content, the alloys kept the same amorphous phase. For Fig. 5b, c, one sharp diffraction peak at $\sim 27.8°$ was corresponded to Na(ReO$_4$) phase, probably due to insufficient washing of the coating after the deposition. With addition of gelatin, the other broad peak at $\sim 27.8°$ was corresponded to carbon phase. The carbon source could result from the adsorption of gelatin on the cathode surface, which was in good agreement with the result of the decrease in current density observed from Fig. 3. Compared with Fig. 5a, the broad diffraction peak for the alloys deposited with gelatin was slightly shifted to the left ($\sim 41.6°$). A slight shift of the peak position was attributed to the incorporation of carbon into the alloys and an increase in Re content. A similar shift has been reported by Yamasaki et al. [22] and Hou et al. [23], in Ni–W alloy structure, which might be attributed to an increase in W content in Ni–W alloys. The average nearest neighbor distance was expanded by the Re atoms incorporated into
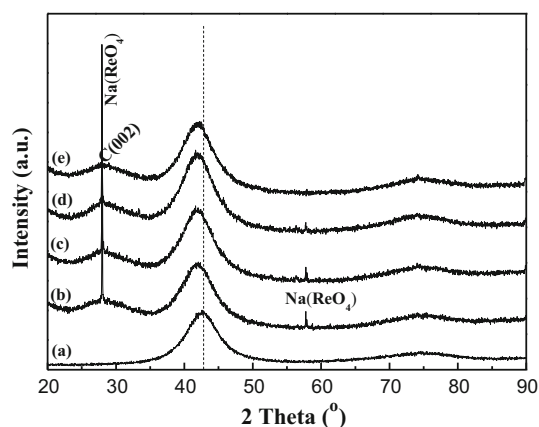
the lattice of Ni and leading to form an amorphous structure.

The morphology of surface of Re–Ni alloys is shown in Fig. 6. As no additive was used, at the surface of the sample appeared smooth, large cracks (ca. ~ 0.9 μm wide) and no pitting (Fig. 6a). Addition of small quantity of gelatin led to cracks and pittings on the surface of the alloy. The formation of cracks may result either from residual stresses or from hydrogen absorption (embrittlement). Some pittings on the surface were attributed to the hydrogen bubbles adsorbed on the surface of cathode metal. With the increase in gelatin contents, the pittings were disappeared. When gelatin content was 0.3 g L^{-1}, some small aggregates were formed (Fig. 6b). The width of cracks was unchanged substantially. When gelatin content was up to 0.9 g L^{-1}, several aggregates were formed (Fig. 6c). Further, lots of aggregates with micrometer size were present on the surface of the alloy with increasing gelatin content. The small cracks (ca. ~ 0.4 μm wide) appeared on the surface. As gelatin content was more than 2.7 g L^{-1}, the morphology of the alloy was almost similar and lots of aggregates were formed. However, the width of cracks did not decrease with increasing gelatin content. The optimum concentration of gelatin was found to be about (0.9–2.7) g L^{-1}. The microstructure evolution of the alloy was changed from smooth and uniform surface to relatively coarse-grained surface containing globule-shaped aggregates. The obvious grain boundaries between the aggregates were observed when gelatin content was above 0.9 g L^{-1}. It was indicated that the presence of gelatin led to significant grain coarsening. On the other hand, the width of cracks decreased with increase in gelatin contents, but the cracks did not completely disappear.

Figure 7 shows the ESEM images of cross section of Re–Ni alloys. It can be observed from Fig. 7a, b that the thickness of the alloys was uniform and homogenous. The coating/substrate interface exhibited good adhesion with no evidence of delamination. The cross section images of the alloys obtained from the bath deposition containing 0.0 and 4 g L^{-1} of gelatin revealed the thickness of approximately 16.4 and 9.2 μm, respectively. Therefore, the deposition rates of the alloys were 16.4 and 9.2 μm h^{-1}, respectively. It was indicated that the deposition rate of the alloy decreased with addition of gelatin.

Figure 8 illustrates the 2D and 3D AFM images of surface of Re–Ni alloys. The scanning scale of images was 10 μm × 10 μm. With absence of gelatin, the R_a and R_q values were 38 ± 13.1 and 49 ± 17.9 nm, respectively. However, with presence of gelatin, the R_a and R_q values were 45 ± 10.3 and 59 ± 15.9 nm, respectively. These data showed the addition of gelatin could result in the increase in surface roughness of the alloy, which was attributed to the effect of grain coarsening. In Fig. 8a, b,
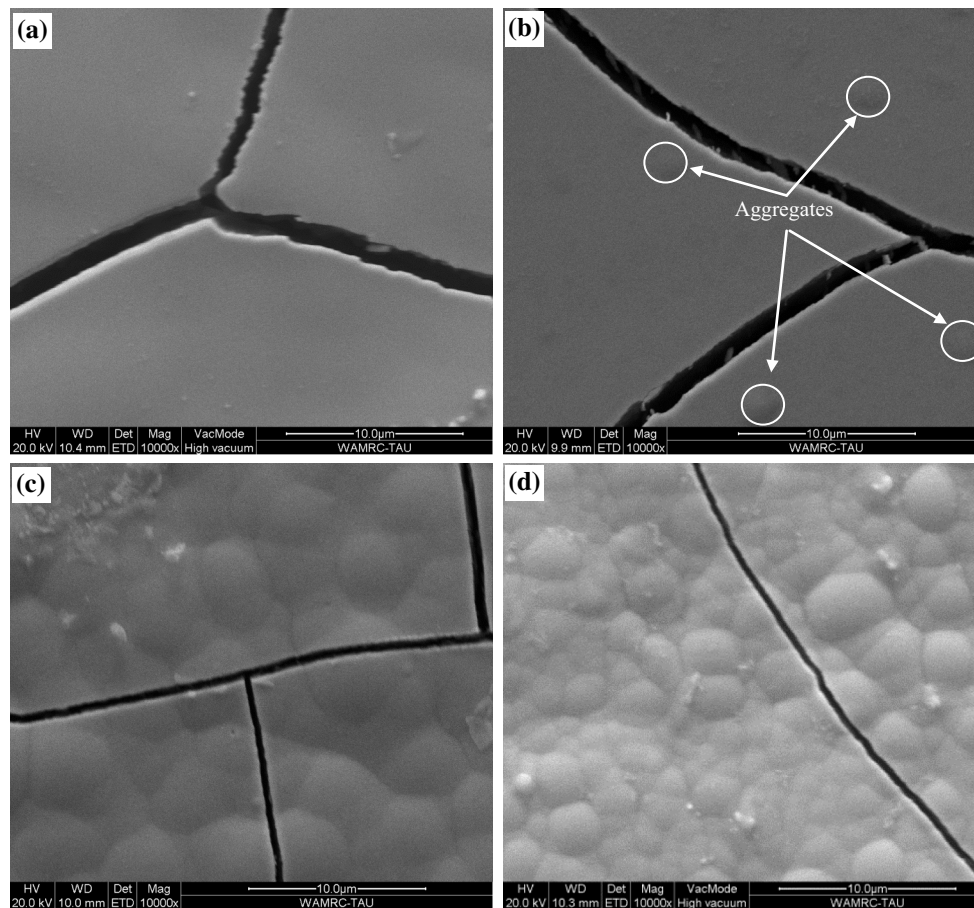

Fig. 5 XRD patterns of Re–Ni alloy coating obtained from the bath deposition containing 0.0 g L^{-1} (**a**), 0.3 g L^{-1} (**b**), 0.9 g L^{-1} (**c**), 2.7 g L^{-1} (**d**) and 3 g L^{-1} (**e**) of gelatin

Fig. 6 ESEM images of surface of Re–Ni alloys **a** 0.0 g L^{-1}, **b** 0.3 g L^{-1}, **c** 0.9 g L^{-1}, **d** 5 g L^{-1}
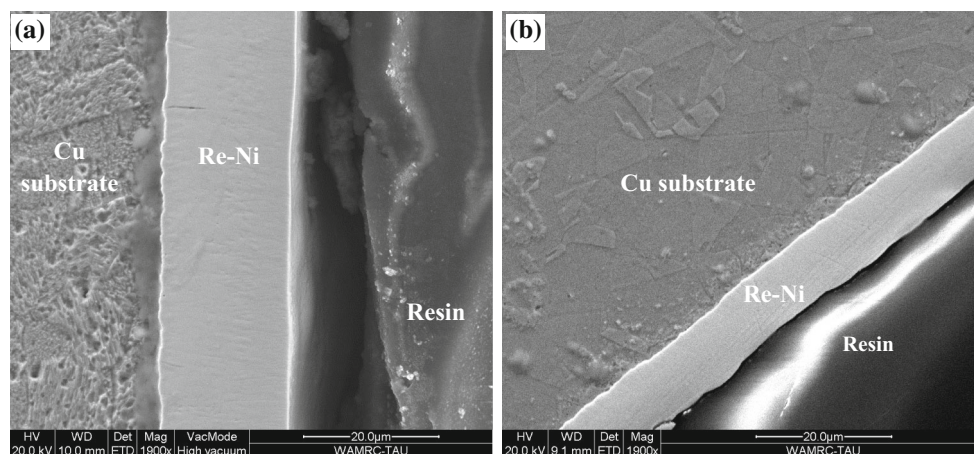

Fig. 7 ESEM images of cross section of the alloys deposited containing 0.0 g L^{-1} (**a**) and 4 g L^{-1} (**b**) of gelatin

the surface of the coating was homogenous, and cracks were present. There was no evidence of obvious grain boundaries on the surface, indicating an amorphous structure. However, cracks and lots of large aggregates were observed (Fig. 8c, d). Fine aggregates emerged among the large coarse grains on the surface. The absence of a periodic structure was evidence, and the presence of random humps supported the existence of an amorphous structure. This result was in good agreement with the observation of XRD pattern.
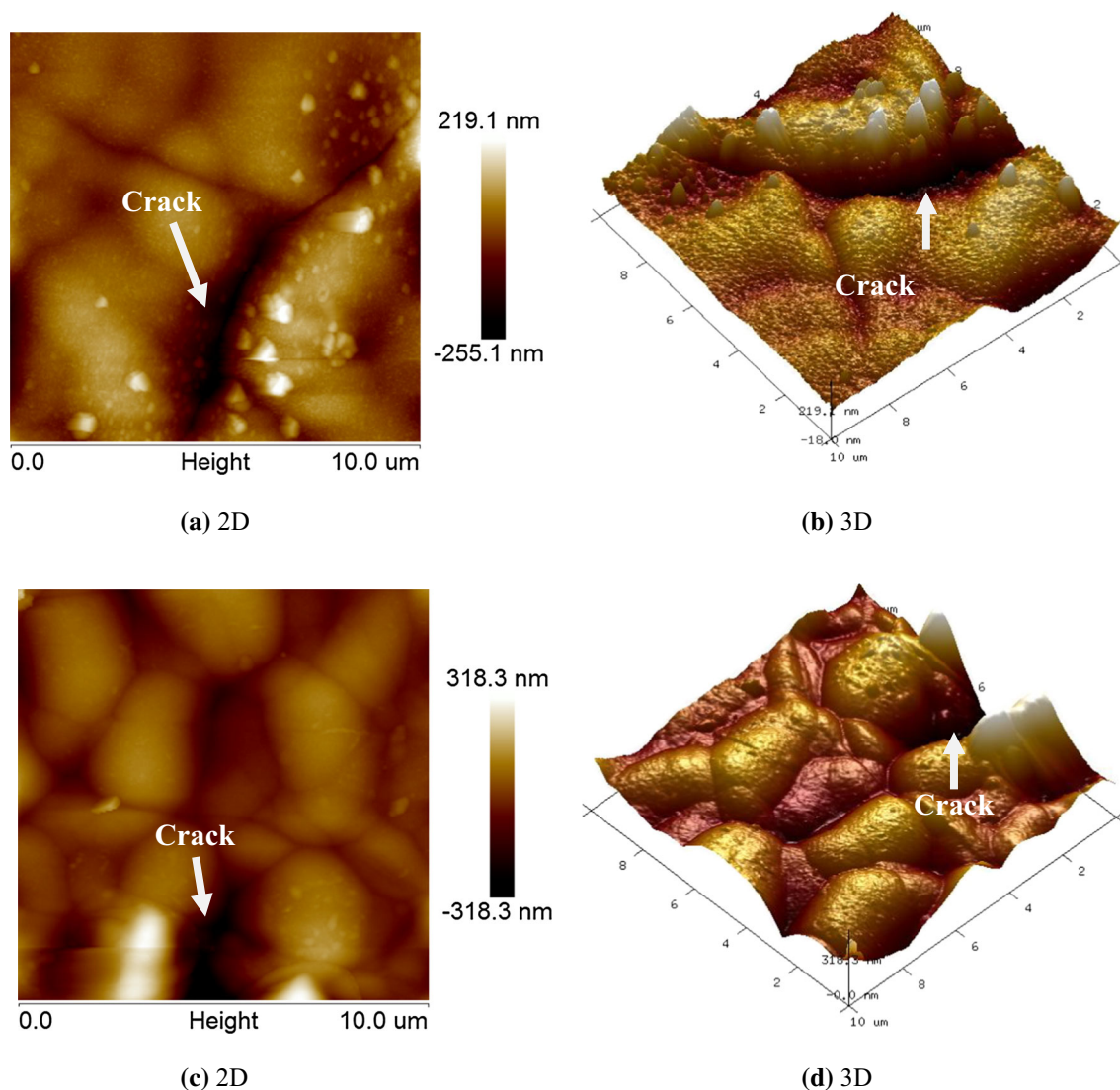
(a) 2D   **(b)** 3D

(c) 2D   **(d)** 3D

Fig. 8 2D and 3D AFM images of surface of Re–Ni alloys obtained from the bath deposition containing 0.0 g L^{-1} (**a** and **b**), 4 g L^{-1} (**c** and **d**) of gelatin

4 Discussion

Gelatin has a triple-helical structure, which is soluble in water at temperature higher than 37.5 °C. In this study, the electrolyte temperature of 70 °C led to a complete denaturation process of gelatin polymolecule and one conversion from a triple-helical structure to a random coil configuration. In the electrolyte, the gelatin molecule was positively charged because pH = 5 was lower than its isoelectric point of ∼9 [24]. After the nucleation of Re–Ni alloy on the cathode surface in the nucleation step, the gelatin adsorbed onto the cathode surface during the first growth stage, preventing the nuclei from further growth and helping in refining the alloy structure [25]. Therefore, the deposition rate of Re–Ni alloy decreased with addition of gelatin due to the increase in viscosity in the gelatin–water

system. In Fig. 2, the addition of gelatin resulted in the high cathode overvoltage in a wide range of gelatin content, causing the nucleation rate to increase [26]. Gelatin contributed in improving the bath stability, possibly by altering electrodeposition potentials and electrolyte viscosity. The addition of gelatin led to grain coarsening on the surface of the alloys, which was due to the re-nucleation of the reduced metals. Therefore, the gelatin suppressed growth rate and so allowed the nucleation rate faster.

The molecule structure of the gelatin consists of a series of different amino acids that link by peptide bonds (See Fig. 1). In the electrolytes, several nitrogen atoms were available for adsorption on the cathode surface and were formed to complex with metal ions [27]. Brown and Hope [28] reported about the adsorption of gelatin on Cu

substrate in sulfuric acid solutions. Adsorption of gelatin on the cathode surface occurred through electron-rich donor atoms such as nitrogen or oxygen. The chemical environment of each of these nitrogen atoms was influenced by neighboring functional groups and the extent of hydrogen bonding in the molecule. The gelatin affected the deposition process through preferential adsorption on the cathode surface. In this study, the presence of gelatin led to an increase in the Re content of Re–Ni alloys. Eliaz et al. [20] suggested that the composition of Zn–Ni alloy was governed by adsorption of gelatin on the cathode surface. Soares et al. [25] suggested that the Ni content of Zn–Ni alloys decreased with the addition of gelatin. In the citrate solutions without gelatin, Naor et al. [7] studied that the increase in Re content of Re–Ni alloys at high citric acid concentration may be related to the formation of $\left[Ni(H_2Cit)_2\right]^0$ or $\left[Ni(HCit)_2\right]^{2-}$ species, which inhibited the parallel paths for deposition of Ni. Gelatin has complex agent ability to coordinate with metallic ions. Kostromina et al. [29] suggested that Ni^{2+} displayed a larger tendency to form bonds with NH groups in the bath containing gelatin at pH of 3–5. To explain the decrease in Ni percentage in the deposits, it was assumed that Ni^{2+} complexes suppressed the reduction of nickel ions in the electrolytes.

The internal stress of a deposit usually consists of extrinsic and intrinsic stresses [30]. Extrinsic stress arises from the lattice differences between the substrate and the deposit. Intrinsic stress is governed by the chemical composition of the electrolyte, deposition temperature, pH and current density [6, 31]. The evident result of stress generation is the formation of cracks. The hydrogen dissolution into the alloys might play an important role of the cracks formation. Hydrogen dissolution in the deposit and its subsequent release was assumed to be the origin of the occurrence of tensile stress [32]. Huang et al. [18] presented that the absorbing hydrogen of the crack-free deposits existed in a stable hydride state. If the amount of absorbing hydrogen was greater than the solubility in the stable hydride state, cracks were formed on the surface of the deposits because the hydride formation became unstable. For the electrodeposited Re film, it was unstable in air and moisture because of the inclusion of Re hydride, and the formation of surface cracks might be due to the presence of the brittle hydride phase [5]. A hexagonal nickel hydride (Ni_2H) was formed in the Re_{48}–Ir_{15}–Ni_{37} alloy, and the crack occurrences might be associated with post-electrolysis decomposition of a hydride phase [15]. In the current study, the addition of gelatin resulted in an increase in the Re content of Re–Ni alloys; the Re or Ni hydride phases should exist in the Re–Ni alloys (See Fig. 5). The density and width of cracks decreased with addition of gelatin of above 2.7 g L^{-1}, because gelatin could lower internal stresses in the deposits by preventing the nuclei from further growth. Some better additives would be looked for the electrodeposition of Re–Ni alloys to reduce the crack formation on the surface of the alloys in aqueous solutions, maybe some additives were used together to eliminate the size and density of cracking for practical requirements.

5 Conclusions

The Re–Ni alloys with high Re content were electrodeposited from aqueous citrate solutions with addition of gelatin. The addition of gelatin had an important influence on electrodeposition of Re–Ni alloys. The measured potential of the alloy was toward more negative value with the addition of gelatin due to the increase in solution viscosity, and further kept constant when the gelatin content was above 2.7 g L^{-1}. In the presence of gelatin, the diffusion limiting current density decreased by about 42 mA cm^{-2} due to the preferential adsorption of gelatin on the cathode surface. The [Re]:[Ni] ratio increased with increasing gelatin contents from 0.0 to 3.0 g L^{-1}, but the FE and partial current densities decreased. As the gelatin concentration was above 3.0 g L^{-1}, the FE, the [Re]:[Ni] ratio and the partial current densities were kept nearly constant. With addition of low concentration of gelatin, the large cracks and pitting were present on the surface. With increasing gelatin content above 0.9 g L^{-1}, a low density of cracks and no pitting appeared, and the gelatin led to significant grain coarsening of the alloys. Compared with the case when no additive was used, the surface roughness of Re–Ni alloys with gelatin increased due to the grain coarsening. The addition of gelatin resulted in the slow deposition rate of the alloys, because gelatin could lower internal stresses in the deposits by preventing the nuclei from further growth. The presence of gelatin resulted in small amount of carbon in the alloys due to the absorption of gelatin. The Re–Ni alloys with high Re content were composed of an amorphous phase. The optimum concentration of gelatin added to a bath containing 34 mM ReO_4^-, 124 mM Ni^{2+} and 343 mM Cit^{3-} was found to be in the range of (0.9–2.7) g L^{-1}.

References

1. T.M. Selvakumari, R.N. Emerson, S. Ganesan, Digest J. Nanomater. Biostruct. **6**, 9 (2011)
2. T.C. Franklin, Surf. Coat. Technol. **30**, 415 (1987)

3. S.R. Brankovic, B. Kagajwala, J. George, G. Majkic, G. Stafford, P. Ruchhoeft, Electrochim. Acta **387**, 83 (2012)
4. M. Paunovic, M. Schlesinger, *Fundamentals of Electrochemical Deposition*, 2nd edn. (Wiley, New York, 2005), pp. 177–198
5. N. Eliaz, E. Gileadi, Induced Codeposition of Alloys of Tungsten, Molybdenum and Rhenium with Transition Metals, in *Modern Aspects of Electrochemistry*, vol. 42, ed. by C.G. Vayenas, R.E. White, M.E. Gamboa-Aldeco (Springer, New York, 2008), p. 191. **(Chapter 4)**
6. A. Naor, N. Eliaz, E. Gileadi, Electrochem. Soc. Trans. **137**, 25 (2010)
7. A. Naor, N. Eliaz, E. Gileadi, Electrochim. Acta **6028**, 54 (2009)
8. A. Naor-Pomeranz, L. Burstein, N. Eliaz, E. Gileadi, Electrochem. Solid-State Lett. **13**, D91 (2010)
9. A. Naor, N. Eliaz, E. Gileadi, J. Electrochem. Soc. **157**, D422 (2010)
10. H. Fukushima, T. Akiyama, M. Shimizu, K. Higashi, Met. Finish. **35**, 247 (1984). **(in Japanese)**
11. H. Fukushima, T. Akiyama, M. Shimizu, K. Higashi, Met. Finish. **36**, 198 (1985). **(in Japanese)**
12. P.R. Zabinski, A. Franczak, R. Kowalik, Arch. Metall. Mater. **57**, 495 (2012)
13. S.K. Mondal, F. Contu, B. Ewers, J.D. Batteas, S.R. Taylor, in *An AFM Evaluation of Rhenium-Nickel Electrodeposit Nucleation on Copper*, 225th ECS Meeting, (2014), p. 530
14. O. Berkh, N. Eliaz, E. Gileadi, J. Electrochem. Soc. **161**, D219 (2014)
15. M. Cohen-Sagiv, N. Eliaz, E. Gileadi, Electrochim. Acta **88**, 240 (2013)
16. A. Duhin, A. Inberg, N. Eliaz, E. Gileadi, Electrochim. Acta **56**, 9637 (2011)
17. V.P. Greco, *Rhenium Alloys-Ion Group Metals-Electrodeposition and Properties*, Technical Report, WVY-7150, 1971. http://www.dtic.mil/dtic/tr/fulltext/u2/741362.pdf
18. C.H. Huang, J.R. Jan, W.Y. Shu, H.M. Wu, Mater. Chem. Phys. **70**, 168 (2001)
19. N. Eliaz, K. Venkatakrishna, A.C. Hegde, Surf. Coat. Technol. **205**, 1969 (2010)
20. R.A. Abuknesha, F. Jeganathan, R. DeGroot, D. Wildeboer, R.G. Price, Anal. Bioanal. Chem. **396**, 2547 (2010)
21. F. Contua, S.R. Taylor, Electrochim. Acta **70**, 34 (2012)
22. K.H. Hou, Y.F. Chang, S.M. Chang, C.H. Chang, Thin Solid Films **518**, 7535 (2010)
23. T. Yamasaki, Scr. Mater. **44**, 1497 (2001)
24. J. Elias, P. Brodard, M.G.C. Vernooij, J. Michler, L. Philippe, Electrochim. Acta **56**, 1485 (2011)
25. L. Oniciu, L. Muresan, J. Appl. Electrochem. **21**, 565 (1991)
26. M.E. Soares, C.A.C. Souza, S.E. Kuri, Mater. Sci. Eng.: A **402**, 16 (2005)
27. L.X. Wei, A.S.M.A. Haseeb, Y.X. Goh, Effects of thiourea and gelatin on the electrodeposition of Sn-Ag solder alloy, in *The 4th Asia Symposium on Quality Electronic Design* (2012) pp. 291–296
28. G.M. Brown, G.A. Hope, J. Electroanal. Chem. **397**, 293 (1995)
29. N.A. Kostromina, S.L. Davydova, A.D. Shaposhnikova, V.P. Tikhonov, Theor. Exp. Chem. **15**, 228 (1979)
30. F. Czerwinski, Thin Solid Films **280**, 199 (1996)
31. N. Eliaz, T.M. Sridhar, E. Gileadi, Electrochim. Acta **50**, 2893 (2005)
32. I. Mizushima, P.T. Tang, H.N. Hansen, M.A.J. Somers, Electrochim. Acta **51**, 6128 (2006)